Title: A regulatory B cell subpopulation expressing CD301b lectin promotes breast cancer growth

Authors: Amy V. Paschall[1]†, Zahra Nawaz[1]†, and Fikri Y Avci[1*]

Affiliations: [1]Department of Biochemistry, Emory Vaccine Center, Winship Cancer Institute, Emory University School of Medicine, Atlanta, GA 30322

†**These authors contributed equally.**

*Corresponding author. Email: favci@emory.edu

Abstract

Tumor-associated carbohydrate antigens (TACAs) can promote tumor growth by regulating the anti-tumor immune response. The accumulation of immune suppressor cells within the tumor in response to TACAs suggests a critical pathway to suppress immune targeting of the tumor. Employing murine breast cancer models, we isolated a regulatory B cell subpopulation in the breast tumor microenvironment that displays an immune suppressive phenotype through its Tn TACA-binding lectin, CD301b. We then demonstrated that depleting CD301b^{+} cells facilitated tumor control and mouse survival, whereas increasing Tn antigen expression decreased mouse survival. As tumor cells use Tn expression to overcome immune targeting, interfering with or blocking the Tn-CD301 axis may unleash the immune system, specifically within the aberrantly glycosylated tumor microenvironment, offering new immunotherapy for breast and other cancers.

MAIN TEXT

Introduction

A major setback observed in many cancers arises from the modulation of the immune system to prevent effective anti-cancer responses. Vaccines, CAR T cells, and checkpoint blockade prime the immune system against cancer-associated antigens, promoting cancer cell destruction via immune cytotoxicity (*1*). Breast cancer is a prime example of a "cold tumor" that doesn't trigger a robust immune response (*2*). Immune therapies for breast cancer remain largely ineffective due to the ability of the tumor to grow unimpeded and eventually metastasize. Immune regulation can occur through cytokine secretion (such as IL-10) (*3, 4*), signaling mechanisms, or checkpoints (such as through PD-1) (*5*). During the malignant transformation of a mammalian cell, a dramatic and aberrant modification of cellular glycosylation is observed. Tumor-associated carbohydrate antigens, or TACAs, can induce immune suppression, allowing cancer cells to evade immune cells (*6-8*). Lectins, such as galectins, are carbohydrate-binding proteins that function as immune cell receptors and can activate immune regulatory pathways through their interactions with TACAs (*9, 10*). Similarly, modulating immune profiles in the tumor microenvironment (TME) by engaging sialic-acid-binding immunoglobulin-like lectins (Siglecs) is a known TACA mechanism (*11-13*). Thus, elucidating the protein-carbohydrate interactions in regulating the immune system within the TME is becoming increasingly important.

Tn antigen is a TACA ranked as a high-priority cancer-associated antigen based on its antigenicity and oncogenicity (*14-18*). Tn is a truncated form of the normal, extended cell surface O-glycan. Tn is the terminal O-linked N-acetylgalactosamine (GalNAc) on serine or threonine residues. The aberrant glycosylation associated with Tn may occur when the enzyme responsible for O-glycan elongation—T-synthase—or its associated chaperone—cosmc (C1GALT1C1)—becomes functionally inhibited (*19, 20*). Tn-expressing mucin 1 (MUC1) has been associated with breast

49 cancer cells (*21, 22*), especially in triple-negative breast cancer (*23, 24*) , and modulating MUC1
50 expression or Tn glycosylation can inhibit tumor growth (*25-27*). However, developing immune
51 responses against Tn-MUC1 has been problematic (*27, 28*).
52
53 CD301, also known as macrophage galactose-type lectin, or MGL, is a C-type lectin receptor (CLR)
54 that binds Tn antigen on the surface proteins (*29*). In mice, the Tn-recognizing homolog to the
55 human CD301 is CD301b, or MGL2 (*30*). CD301b has been considered to be expressed exclusively
56 by myeloid cells such as dendritic cells (DCs) and macrophages (*17*). Previously, MGL2-expressing
57 myeloid cell populations have been linked with immunosuppressive responses (*16, 17, 31-33*). DCs
58 and macrophages were shown to suppress the proliferation of $CD4^+$ effector T lymphocytes through
59 the interaction of MGL with terminal GalNAc residues on CD45 expressed by T cells (*17*). This
60 cell-specific glycosylation of CD45 provided an immunoregulatory pathway of MGL-mediated
61 control of T_{eff} cell function. In another study, $CD301b^+$ dendritic cells were shown to suppress T
62 follicular helper cells and antibody responses to protein antigens (*31*). Recently, an
63 immunosuppressive DC subset expressing CD301b was shown to accumulate at secondary sites
64 and promote metastasis in pancreatic cancer (*33*) and lung cancer (*34*).
65
66 Here, we demonstrate the accumulation of $CD301b^+$ immune cells in the tumor microenvironment
67 as a response to Tn-expression by breast cancer cells. We characterize these cells into populations
68 of cells expressing markers associated with regulatory innate-like B cells and produce suppressive
69 cytokines. As a subset of B lymphocytes, regulatory B cells (Bregs) exhibit immunosuppressive
70 functions in homeostasis (*35*) and numerous disease states, including colitis (*36*), arthritis (*37*), HIV
71 (*38, 39*), and multiple cancers (*40-43*). Thus, these cells are broadly relevant in multiple tissues,
72 systems, and microenvironments throughout the body (*35*). Breg cells are typically characterized
73 by their production of IL-10 (*37, 44*), a cytokine most frequently implicated in immune suppression.

74 Inhibiting IL-10-producing Bregs has been shown to disrupt normal anti-inflammatory processes
75 and can result in chronic inflammation (*45*). Bregs are often identified by key cell surface markers,
76 including CD1d(*46*), CD24 (*47*), and/or CD5 (*46*). A heterogeneous subpopulation of B cells
77 expressing innate cell markers such as CD11b and demonstrating immunoregulatory functions has
78 been identified (*37, 45, 48-54*). Of note, a subpopulation of innate-like B cells may produce high
79 levels of IgM as one mechanism for decreasing inflammatory responses (*55*).
80
81 This work offers a method of immune suppression similar to checkpoint regulation, which has
82 represented critical targets in the rapidly advancing field of cancer immunotherapy. Immune
83 interactions of TACAs have been severely understudied. Elucidating immune suppression
84 mechanisms through protein-carbohydrate interactions has important implications for discovering
85 new immune therapies to boost immune anti-cancer function through overcoming regulation
86 mechanisms.
87
88 **Results**
89
90 ***CD301b$^+$ cells accumulate in a murine breast cancer model***
91 We first sought to establish the relationship between CD301b$^+$ immune cells and Tn glycoantigen-
92 expressing breast cancer cells. We used a CRISPR-Cas9 gene editing model to knockout cosmc
93 chaperone expression in AT3 murine breast cancer cells. Cosmc is a chaperone essential in
94 elongating the core O-glycan beyond the truncated Tn form of α-GalNAc (*19, 20, 56*). When cosmc
95 function/expression is disrupted, elongation of the O-glycan is not observed; instead, the Tn antigen
96 is observed at significantly higher levels. After disrupting cosmc expression in these cell lines, we
97 confirmed increased Tn cell surface expression through flow cytometry using both a reBaGs6 IgM
98 antibody (Supplementary Fig. 1A) (*57*) as well as a complementary biotinylated VVL lectin
99 coupled with fluorescent streptavidin (Supplementary Fig. 1B). Both staining methods indicated

100 significantly higher Tn expression on the cosmc KO cell line. We also isolated RNA from each cell
101 line and confirmed decreased cosmc expression in the Tn^{hi} cell line through qPCR using cosmc
102 primers (Supplementary Fig. 1C). We then tested whether knocking out cosmc expression changes
103 the proliferation rate of the AT3 breast cancer cells *in vitro*. After culturing both cell lines at the
104 same concentrations for three days, we observed no significant differences in cell proliferation
105 between the two lines (Supplementary Fig. 1D), indicating that Tn expression alone does not
106 promote cancer cell growth.
107 To determine the *in vivo* tumor cell growth, we injected AT3 (Tn^{lo}) and AT3 cosmc KO (Tn^{hi})
108 murine breast tumor cells into the mammary pads of C57BL/6 mice (n=25) and monitored tumor
109 growth for up to 23 days. We observed that Tn^{hi} tumors grew significantly faster than Tn^{lo} tumors
110 (Fig. 1A), indicating that Tn expression impacts tumor growth rate. Tumor-bearing and tumor-free
111 control mice were then euthanized to assess CD301b on multiple immune cell subsets in the spleen,
112 draining lymph nodes (or analogous lymph nodes in tumor-free mice), bone marrow, or breast
113 tumors by flow cytometry (for gating strategy, please see Supplementary Fig. 2). A significantly
114 higher accumulation of $CD45^{+}CD301b^{+}$ immune cells was observed in the Tn^{hi} tumor
115 microenvironments compared to the Tn^{lo} tumor tissue (Fig. 1B-C). Low levels of cell surface
116 CD301b were observed on immune cell subsets in the spleens or lymph nodes of tumor-free mice
117 (Fig. 1C). However, a significant population of $CD45^{+}CD301b^{+}$ cells was observed in the tumor
118 tissues and the bone marrow of the tumor-bearing mice. $CD301b^{+}$ immune cell accumulation in the
119 TME correlates with tumor Tn expression.
120

121 ***Tumor-infiltrating CD301b^{+} cells display a regulatory B-cell phenotype***

122 We next observed that essentially all tumor-infiltrating $CD45^{+}CD301b^{+}$ immune cells express the
123 B-cell markers B220 and CD19, and they do not express markers associated with other major
124 immune cell types CD3, NK1.1 and CD11c (Fig. 2A-D). CD11b expression on the tumor-

125 infiltrating $CD45^{+}CD301b^{+}$ varied (Fig. 2B, 2D). Since CD301b function has primarily been
126 attributed to myeloid cells, and particularly to DCs, we assessed and observed that the tumor-
127 infiltrating CD45+CD301b+B220+CD19+ immune cells do not express CD11c (Fig. 2E). The
128 absolute number of B220+CD19+ cells per mg of tumor tissue is highly increased in Tn^{hi} tumor
129 tissues compared to Tn^{lo} tumors, with approximately a third of them expressing CD301b+ in the
130 Tn^{hi} tumors (Fig. 2F).
131
132 The tumor-infiltrating $B220^{+}CD19^{+}CD301b^{+}$ cells express cell surface IgM, a B cell-specific
133 surface receptor (Fig. 3A). Next, we observed the $CD301b^{+}$ B cells express surface proteins
134 associated with regulatory B cells, such as CD5, CD24, Gr1 with varying levels, while other surface
135 markers traditionally associated with Bregs (CD1d, CD25, CD21, Ly6C and Ly6G) were minimally
136 expressed on these $B220^{+}CD19^{+}CD301b^{+}$ B cells (Fig. 3B-F). The tumor-infiltrating $CD301b^{+}$ cells
137 may represent a previously uncharacterized subset of B cells with a phenotype indicating an innate-
138 like regulatory B cell population (*48-55*).
139
140 ***Tn-Expressing Cancer Cells Induces Expression of CD301b on B cells***
141 CD301b mean fluorescence intensity (MFI) was significantly higher in Tn^{hi} tumor-infiltrating cells
142 than Tn^{lo} (Fig. 3G), indicating that CD301b expression is tumor Tn-associated. To further elucidate
143 if B cells can express CD301b in response to Tn expression, we obtained splenocytes from healthy
144 WT C57Bl/6 mice and used magnetic cell sorting protocols to positively select for $CD19^{+}$ cells or
145 isolate pan B cell populations through negative selection, compared to unselected total splenic
146 mononuclear cells (Supplementary Fig. 3). These splenocyte populations were then co-cultured
147 with either AT3 Tn^{lo} or AT3 Tn^{hi} cancer cells, compared to cultured alone (unstimulated). After
148 three days of co-culture, cells were analyzed using flow cytometry: viable singlet
149 $CD45^{+}B220^{+}CD19^{+}$ cells were gated out, and CD301b MFI was assessed in each group. We

150 observed significantly higher CD301b expression in all splenocyte groups co-cultured with Tn^{hi}
151 cancer cells compared with unstimulated or Tn^{lo} cancer cell co-cultures (Fig. 3H). These results
152 indicate an important role for Tn in the expression of CD301b on B cell populations.
153

154 ***B Cell Deficient Mice did not Exhibit CD301b+ Cell Accumulation in Response to Tn^{hi} Tumor***

155 Towards elucidating the role of CD301b+ B cells in the context of Tn-expressing tumor growth,
156 we used RAG1 KO (B6.129S7-Rag1tm1Mom/J) mice that lack functional T or B cells. We injected
157 Tn^{hi} tumor cells into the mammary pads of RAG1 KO mice alongside a WT control group. We
158 observed significantly decreased tumor growth (Fig. 4A) and no observable CD301b+ immune cells
159 infiltrating the tumors (Fig. 4B-C) compared to WT mice. No observable B220+CD19+ cells were
160 present within the RAG1 KO mouse tumors (Fig. 4D). These results further demonstrate that the
161 tumor-infiltrating CD301b+B220+CD19+IgM+ immune cells constitute a B cell population as they
162 are absent when mice lack the lymphocyte-specific *rag1* gene. Our results also suggest that
163 CD301b+ B cells play a regulatory function in promoting tumor growth. However, along with the
164 CD301b+ B cells, all lymphocytes, including T cells and CD301b- B cells, are absent in RAG1 KO
165 mice. Therefore, attributing such an immunoregulatory role to tumor-infiltrating CD301b+ B cells
166 requires elucidating their functional properties specifically, as laid out in the next two sections.
167

168 ***Tumor-infiltrating $CD301b^{+}$ B cells exhibit immunosuppressive characteristics***

169 To better understand the functional suppressive characteristics of tumor-infiltrating CD301b+ B
170 cells, we used intracellular staining of Tn^{hi} breast tumor-bearing mouse tumor tissue to stain for
171 regulatory cytokines. We gated and compared the following populations: $CD45^{+}B220^{+}CD19^{+}$ B
172 cells in tumor-free spleens and $CD45^{+}CD301b^{+}B220^{+}CD19^{+}$ from Tn^{hi} tumors. Of note, we
173 observed that tumor-associated $CD19^{+}B220^{+}CD301b^{+}$ produce significantly higher levels of IL10,
174 TGFβ, and subunits of IL35 than splenic-derived B cells from tumor-free mice as controls (Fig.

175 5A-B, Supplementary Fig. 4), suggesting a role for immune suppression in this tumor-infiltrating
176 B cell subset.
177
178 ***CD301b/Tn Axis Impacts Tumor Growth and Mouse Survival***
179 To illuminate how CD301b immune cells contribute to tumor growth, we employed a mouse model
180 in which CD301b immune cells can be depleted: B6(FVB)-*Mgl2*$^{tm1.1(HBEGF/EGFP)Aiwsk}$/J mice
181 (MGL2-DTR)(*31, 32*). We injected AT3 Tn^{lo} or Tn^{hi} tumor cells (Fig. 6A) into MGL2-DTR mice
182 that were/ were not CD301b-depleted with diphtheria toxin treatment. We measured tumor growth
183 and observed a significant decrease in tumor size when CD301b^{+} immune cells were depleted in
184 the Tn^{hi} group. We also injected AT3 Tn^{hi} cells into mammary pads of CD301b null MGL2-DTR
185 homozygous mice and observed significantly lower breast tumor growth than WT mice (Fig. 6B).

186 In a complementary experiment, we used a mouse model expressing human MUC1: C57BL/6-
187 Tg(MUC1)79.24Gend/J (*58*). These mice display aberrant glycosylation on MUC1, such as Tn
188 antigen, unlike wild-type mouse MUC1 glycosylation (*59-62*). We used methylcholanthrene
189 (MCA) as a carcinogen to induce spontaneous tumors in the mammary pads of both WT and
190 Muc1.Tg mice to assess how Tn expression affects tumor growth. We observed significantly
191 increased tumor growth rates to endpoint tumor sizes over 21 weeks in the Muc1.Tg mice (Fig.
192 6C), indicating that higher Tn expression on spontaneous tumors—not just cancer cell lines—can
193 impact breast cancer prognosis. To our point, tumor-infiltrating B cells from MUC1.Tg
194 spontaneous tumors showed significantly higher percentages of CD301b^{+} cells than the
195 corresponding B cell populations from WT MCA-induced tumors (Fig. 6D). These data together
196 indicate an important role for the CD301b-Tn axis in breast tumor development and the high
197 therapeutic potential for modulating it to improve the anti-tumor immune response in breast cancer.
198 However, other factors, such as differences in tumorigenicity, cell-intrinsic tumor growth, or
199 metastatic activity, can potentially contribute to the difference in survival in conjunction with or

200 independent from the interaction of MUC1-Tn with CD301b+ cells. Modulating CD301b and Tn
201 expression in this mouse model would enable further evaluation of the CD301b-Tn axis in tumor
202 immunoregulation.

203 **Discussion**

204 Numerous recent research studies have established the importance of Tn as a key antigen in relation
205 to human cancer development and progression (*20, 21, 63-65*). Additionally, CD301 plays an
206 immune regulatory role in human infection (*31, 32*) and the progression of human cancer (*33*). In a
207 recent study, CD301b^{+} DCs were shown to accumulate in response to higher levels of Tn in lung
208 tumor cells, and the Tn-CD301b interactions influence the development of pro-angiogenic
209 programs (*34*). The link between Tn and CD301-mediated immune responses thus needs further
210 elucidation, particularly in cancer models known to express aberrant glycosylation, such as breast
211 cancer. Overcoming immune regulation in breast cancer can potentially turn these "cold" tumors
212 into immunotherapeutic-responsive "hot" tumors, potentially improving clinical responses to
213 checkpoint blockade and tumor antigen vaccines. This study shows an accumulation of CD301b^{+}
214 immune cells in response to high Tn antigen expression by developing breast tumors in mice. These
215 CD301b^{+} immune cells phenotypically and functionally display an innate-like B cell phenotype
216 with regulatory functions, including producing immunoregulatory cytokines. Innate-like B cells
217 may express CD11b and CD5 but low levels of CD11c (*53, 66*). Innate-like B cells are also
218 associated with high levels of IgM and low levels of IgD (*55*) These cells have been shown to
219 produce natural IgMs in response to tumor-associated gangliosides (*67*). Of note, extensive research
220 studies have shown that B cells with regulatory function cannot currently be defined based on any
221 specific combination of extracellular markers or transcription factors; rather, the heterogeneity of
222 regulatory B cells suggests that these cells arise in response to environmental stimuli (*35*). We
223 observe suppressive CD301b^{+} cells accumulating in the tumor microenvironment specifically, and
224 particularly in response to higher Tn expression by the developing breast tumor. However, as some

accumulation is observed in bone marrow in tumor-bearing mice, studies investigating the origin of these cell populations would be warranted. MGL2/CD301b function has primarily and predominantly been attributed to myeloid cells in the past decades. Our results indicating that a previously uncharacterized regulatory CD301b+ lymphoid cell population plays an important role in the tumor immune escape warrants further exploration of the function and regulation of *mgl2* gene expression. Particularly, the results obtained in the RAG1 KO mouse model would suggest that CD301b+ B cells promote tumor growth. However, the direct role of B cell-specific CD301b and/or CD301b+ B cells could be further assessed by modulating CD301b expressing cells and B cells independently, such as developing a muMt-/Mgl2-DTR chimeric mouse model.

The MUC1.Tg mouse model is limited because it may not account for CD301b-Tn interaction alone and likely exhibits distinct tumor microenvironment development. Understanding the innate-like characteristics of these cells could have implications for their mechanisms of suppressive functions in the context of Tn^{hi} tumors. Analysis (e.g., via transcriptomics) of these tumor-infiltrating cell populations in relation to the tumor immune microenvironment could thus describe the novel population of suppressive cells and their mechanisms of action. Eliminating these cells can improve tumor response in mice, which has important implications for targeting the CD301b-Tn axis to improve immunotherapy. Further characterization of how these cells modulate immune responses in the TME will help determine optimal therapies to target and overcome their accumulation and immunosuppressive mechanisms. Furthermore, therapies targeting CD301 and/or Tn could improve breast cancer response to breakthrough therapies, such as PD-1 or CTLA-4 checkpoint blockade. Future investigation of these therapeutic strategies will thus be a priority in this research. Understanding how these $B220^{+}CD19^{+}IgM^{+}CD301b^{+}$ immune cells modulate the immune pathways in TME and impact disease progression could have important implications for cancer immunotherapy.

Materials and Methods

251

252 ***Mice***

253 Eight-week-old female C57BL/6 mice were obtained from Jackson Laboratories (Bar Harbor, ME)
254 and housed at Emory University Whitehead Biomedical Research Building. MGL2-DTR mutant
255 mice (*Mgl2*$^{tm1.1(HBEGF/EGFP)Aiwsk}$) were a generous gift from Akiko Iwasaki at Yale University.
256 Muc1.Tg mice (C57BL/6-Tg(MUC1)79.24Gend/J) were a generous gift from Sandra Gendler at
257 Mayo Clinic. Mice were kept in microisolator cages and handled under biosafety level 2 (BSL2)
258 hoods. For tissue processing and subsequent flow cytometry, mice were euthanized by carbon
259 dioxide inhalation in accordance with IACUC guidelines. For applicable experiments, serum
260 samples, spleens, lymph nodes, bone marrow, and/or tumors were harvested. Where applicable, cell
261 suspensions were generated through mechanical tissue disruption and collagenase D digestion. Red
262 blood cells were lysed, and samples were filtered through 60 μm nylon filters to obtain single-cell
263 suspensions. For depletion of CD301b^{+} cells, heterozygous MGL2-DTR mice were treated with
264 diphtheria toxin (0.5μg/mouse) in sterile PBS intraperitoneally every two to three days, starting at
265 day -1 before tumor injection. Effective MGL2 cell depletion was confirmed using flow cytometry
266 in bone marrow and tumor samples (Supplementary Fig. 5A-B). For RAG1 KO experiments, 6-8
267 weeks old RAG1 KO mice (B6.129S7-Rag1tm1Mom/J) were obtained from Jackson Laboratory.
268 The lack of B cell populations was confirmed using flow cytometry in bone marrow and lymph
269 node samples (Supplementary Fig. 5C).

270

271 All mouse experiments were in compliance with the Emory University Institutional Animal Care
272 and Use Committee under an approved animal use protocol. Our animal use protocol adheres to the
273 principles outlined in *U.S. Government Principles for the Utilization and Care of Vertebrate*
274 *Animals Used in Testing*, *Research and Training*, the Animal Welfare Act, the *Guide for the Care*
275 *and Use of Laboratory Animals*, and the *AVMA Guidelines for the Euthanasia of Animals*.

276

277 ***Generation of Tn^{hi} breast cancer cells***

278 To express Tn glycans at high levels in tumor cells, we used a CRISPR/Cas9 methodology to stably
279 silence cosmc expression in AT3 cells using established protocols and reagents. Mouse cosmc guide
280 RNA and CRISPR/Cas9 plasmid were obtained from Santa Cruz Technology (sc-425587). AT3
281 murine breast cancer cells were a generous gift from the Kebin Liu lab at Augusta University. AT3
282 cells were transfected with cosmc CRISPR/Cas9 KO plasmid according to the manufacturer's
283 protocol. Puromycin was used to select transfected cells. We then used flow cytometry to confirm
284 higher expression of Tn on the AT3 cell surfaces using the ReBaG6 antibody (generously provided
285 by Richard Cummings at Harvard University) (Supplementary Fig. 1A) (*57*) and VVL lectin
286 (Vector Laboratories) (Supplementary Fig. 1B). The proliferation of each transfected cell line (AT3
287 and AT3 Tn^{hi}) was tested in an MTT proliferation assay for three days, and colorimetric analysis
288 was performed with a CytoTek plate reader according to protocol; no significant differences in
289 proliferation compared to parent cells were observed (Supplementary Fig. 1D). Cell lines were
290 maintained in RPMI media supplemented with 10% FBS, sodium pyruvate, HEPES buffer, NEAA,
291 β-mercaptoethanol, and penicillin/streptomycin at 37°C, 5% CO2.

292

293 ***AT3 Tn^{lo} and/or AT3 Tn^{hi} Tumor Challenge***

294 Breast tumor cells were harvested and washed in sterile PBS. Cells were suspended in a final
295 concentration of 2.5E6/ml sterile PBS. Cells were subcutaneously injected into the mammary pads
296 of mice at 2.5E5/100µl/mouse. Mice were observed and euthanized at the tumor endpoint
297 (maximum tumor dimension between 0.9 cm and 1.2 cm, typically after Day 17). For instance, Tn^{lo}
298 tumor-bearing mice analyzed for Fig. 2 were sacrificed on Day 23, and Tn^{hi} tumor-bearing mice
299 were sacrificed on Day 17. RAG1 KO mice in Fig. 4 were sacrificed on Day 23. In cases where
300 tumors were observed to ulcerate or reach maximum growth sooner than the earliest endpoint

301 (before Day 17), the mice were euthanized immediately, and samples were excluded. Tumor
302 volumes were calculated as ((length x width x width)/2) in mm^3.
303
304 ***Flow Cytometry***
305 Cells were stained in PBS with TruStain fcX (BioLegend, Cat. No. 101320) to reduce non-specific
306 antibody binding. Cell samples were stained with the following antibodies and stains (in multiple
307 sets to prevent fluorophore overlap): B220-FITC (BioLegend, clone RA3-6B2), CD11c-PacBlue
308 (BioLegend, clone N418), CD11b-FITC (BioLegend, clone M1/70), CD3e-APC (BioLegend, 145-
309 2C11), CD45-APCCy7 (BioLegend, clone 30-F11), CD19-PE (BioLegend, clone 6D5), NK1.1-
310 PerCP (BioLegend, PK136), Gr1-PECy5 (BioLegend), CD19-APC (BioLegend, clone 1D3),
311 Ly6C-BV605 (BioLegend, clone HK1.4), CD11b-PacBlue (BioLegend M1/70), LycG-BV605
312 (BioLegend clone RTK2758), CD1d-PacBlue (BioLegend, clone 1B1), CD5-PECy5 (BioLegend,
313 clone 53-7.3), CD24-PECy7 (BioLegend, clone 30-F1), CD301b-APC (BioLegend, clone URA-1),
314 CD301b-PE (BioLegend, clone URA-1), CD25-BV605 (BioLegend, clone PC61), CD21-BV510
315 (BioLegend), IL10 PECy7 (BioLegend, clone JES5-16E3), TGFb-BV421 (BioLegend, clone TW7-
316 16B4), IgM-PECy5 (BioLegend, clone RMM-1), IgD-PECy7 (BioLegend, clone 11-26c.2a)
317 IL35:EBI3 subunit – PerCP (R&D, clone 355022), IL35:p35 subunit – AF594 (R&D, clone 27537),
318 and Ghost Red 710 (Tonbo Biosciences). For intracellular staining, cell samples were treated with
319 GolgiStop for four hours prior to the staining protocol. Intracellular staining was performed
320 according to the protocol (BD Biosciences). All isotype controls were obtained from BioLegend
321 except isotypes for IL35 subunits, which were obtained from R&D. Samples were washed and
322 analyzed with flow cytometry (Cytek Aurora or Agilent Novocyte Penteon). Fluorescence minus
323 one (FMO) plus specific isotype control antibody-stained samples were used as negative staining
324 controls, and single stains were used for compensation. Flow cytometry data were analyzed using

325 FlowJo Single Cell Analysis Software (Treestar, Inc., Ashland, Oregon) with gating strategies
326 shown in Supplementary Fig. 2 (example showing tumor tissue from Tn^{hi}-tumor bearing mice).
327

328 ***Splenocyte B Cell Selection and Co-Culture***

329 Splenocytes were obtained from healthy WT C57Bl/6 mice. BioLegend MojoSort antibody kits
330 were used to positively select CD19 cells or negatively isolate Pan B cells, according to
331 manufacturer protocols. Flow cytometry was used to determine the B cell purity of each sample
332 (Supplementary Fig. 3). Viable cells were counted and cultured in 96-well plates at 1E5 cells/100 µl
333 complete RPMI (supplemented with Ca+) /well. Tumor cells were harvested, and viable cells were
334 counted. Indicated cell populations were then plated in each splenocyte sample at 1E5 cells/100 µl
335 complete RPMI (for the "Unstimulated" sample, 100 µl complete RPMI was used without tumor
336 cells), for a final volume of 200 µl /well. Plates were cultured for 3 days at 37°C, 5% CO2. Samples
337 were washed and prepared for flow cytometry analysis.
338

339 ***Statistical Analysis***

340 GraphPad Prism v8 was used for statistical analyses. Two-way ANOVA with Tukey's multiple
341 comparisons test was used to determine statistical significance between experimental groups in
342 each of the applicable experimental models (Fig. 1C, Fig. 2F, Fig. 4D, Fig. 6A). Ordinary one-way
343 ANOVA with Tukey's multiple comparisons test was used to analyze Fig. 5. Mouse survival in
344 Fig. 6C was compared using Log-rank (Mantel-Cox) test. An unpaired parametric two-tailed t-test
345 was used for Figs. 1A, 3G, 4A, 4C, 6B, 6D. Significance is indicated on each graph based on p-
346 value: >0.05 = ns; <.05 = *; <0.01 = **; <0.001 = ***; <0.0001 = ****.
347
348
349
350
351
352

353 **References**

354 1. Y. Zhang, Z. Zhang, The history and advances in cancer immunotherapy: understanding the
355 characteristics of tumor-infiltrating immune cells and their therapeutic implications. *Cell Mol*
356 *Immunol* **17**, 807-821 (2020).
357 2. A. Swoboda, R. Nanda, Immune Checkpoint Blockade for Breast Cancer. *Cancer Treat Res* **173**,
358 155-165 (2018).
359 3. D. F. Fiorentino, M. W. Bond, T. R. Mosmann, Two types of mouse T helper cell. IV. Th2 clones
360 secrete a factor that inhibits cytokine production by Th1 clones. *J Exp Med* **170**, 2081-2095
361 (1989).
362 4. S. E. Acuner Ozbabacan, A. Gursoy, R. Nussinov, O. Keskin, The structural pathway of interleukin 1
363 (IL-1) initiated signaling reveals mechanisms of oncogenic mutations and SNPs in inflammation
364 and cancer. *PLoS Comput Biol* **10**, e1003470 (2014).
365 5. G. J. Freeman *et al.*, Engagement of the PD-1 immunoinhibitory receptor by a novel B7 family
366 member leads to negative regulation of lymphocyte activation. *J Exp Med* **192**, 1027-1034 (2000).
367 6. N. Rodrigues Mantuano, M. Natoli, A. Zippelius, H. Laubli, Tumor-associated carbohydrates and
368 immunomodulatory lectins as targets for cancer immunotherapy. *J Immunother Cancer* **8**, (2020).
369 7. H. Laubli, A. Varki, Sialic acid-binding immunoglobulin-like lectins (Siglecs) detect self-associated
370 molecular patterns to regulate immune responses. *Cell Mol Life Sci* **77**, 593-605 (2020).
371 8. S. S. Pinho, C. A. Reis, Glycosylation in cancer: mechanisms and clinical implications. *Nat Rev*
372 *Cancer* **15**, 540-555 (2015).
373 9. K. V. Marino, A. J. Cagnoni, D. O. Croci, G. A. Rabinovich, Targeting galectin-driven regulatory
374 circuits in cancer and fibrosis. *Nat Rev Drug Discov* **22**, 295-316 (2023).
375 10. A. J. Cagnoni *et al.*, Galectin-1 fosters an immunosuppressive microenvironment in colorectal
376 cancer by reprogramming CD8(+) regulatory T cells. *Proc Natl Acad Sci U S A* **118**, (2021).
377 11. R. Beatson *et al.*, The mucin MUC1 modulates the tumor immunological microenvironment
378 through engagement of the lectin Siglec-9. *Nat Immunol* **17**, 1273-1281 (2016).
379 12. N. T. Marcos *et al.*, Role of the human ST6GalNAc-I and ST6GalNAc-II in the synthesis of the
380 cancer-associated sialyl-Tn antigen. *Cancer Res* **64**, 7050-7057 (2004).
381 13. M. J. Schultz *et al.*, The Tumor-Associated Glycosyltransferase ST6Gal-I Regulates Stem Cell
382 Transcription Factors and Confers a Cancer Stem Cell Phenotype. *Cancer Res* **76**, 3978-3988
383 (2016).
384 14. A. V. M. Paschall, D. R.; Avci, F. Y, in *Encyclopedia of Cell Biology, Second Edition,* R. A. H.
385 Bradshaw, G. W.; Stahl, P. D., Ed. (Elsevier, 2023), pp. 404-413.
386 15. T. Freire, R. Lo-Man, S. Bay, C. Leclerc, Tn glycosylation of the MUC6 protein modulates its
387 immunogenicity and promotes the induction of Th17-biased T cell responses. *J Biol Chem* **286**,
388 7797-7811 (2011).
389 16. E. Saeland *et al.*, The C-type lectin MGL expressed by dendritic cells detects glycan changes on
390 MUC1 in colon carcinoma. *Cancer Immunol Immunother* **56**, 1225-1236 (2007).
391 17. S. J. van Vliet, S. I. Gringhuis, T. B. Geijtenbeek, Y. van Kooyk, Regulation of effector T cells by
392 antigen-presenting cells via interaction of the C-type lectin MGL with CD45. *Nat Immunol* **7**, 1200-
393 1208 (2006).
394 18. M. A. Cheever *et al.*, The prioritization of cancer antigens: a national cancer institute pilot project
395 for the acceleration of translational research. *Clin Cancer Res* **15**, 5323-5337 (2009).
396 19. Y. Wang *et al.*, Cosmc is an essential chaperone for correct protein O-glycosylation. *Proc Natl*
397 *Acad Sci U S A* **107**, 9228-9233 (2010).
398 20. T. Ju, R. P. Aryal, M. R. Kudelka, Y. Wang, R. D. Cummings, The Cosmc connection to the Tn
399 antigen in cancer. *Cancer Biomark* **14**, 63-81 (2014).
400 21. R. Beatson *et al.*, The Breast Cancer-Associated Glycoforms of MUC1, MUC1-Tn and sialyl-Tn, Are
401 Expressed in COSMC Wild-Type Cells and Bind the C-Type Lectin MGL. *PLoS One* **10**, e0125994
402 (2015).
403 22. R. E. Beatson, J. Taylor-Papadimitriou, J. M. Burchell, MUC1 immunotherapy. *Immunotherapy* **2**,
404 305-327 (2010).

405 23. A. Siroy *et al.*, MUC1 is expressed at high frequency in early-stage basal-like triple-negative breast
406 cancer. *Hum Pathol* **44**, 2159-2166 (2013).
407 24. J. M. Burchell, R. Beatson, R. Graham, J. Taylor-Papadimitriou, V. Tajadura-Ortega, O-linked
408 mucin-type glycosylation in breast cancer. *Biochem Soc Trans* **46**, 779-788 (2018).
409 25. D. Chen *et al.*, Immunotherapy of spontaneous mammary carcinoma with fusions of dendritic
410 cells and mucin 1-positive carcinoma cells. *Immunology* **109**, 300-307 (2003).
411 26. P. Mukherjee *et al.*, MUC1-specific immune therapy generates a strong anti-tumor response in a
412 MUC1-tolerant colon cancer model. *Vaccine* **25**, 1607-1618 (2007).
413 27. V. Lakshminarayanan *et al.*, Immune recognition of tumor-associated mucin MUC1 is achieved by
414 a fully synthetic aberrantly glycosylated MUC1 tripartite vaccine. *Proc Natl Acad Sci U S A* **109**,
415 261-266 (2012).
416 28. L. R. Loureiro *et al.*, Challenges in Antibody Development against Tn and Sialyl-Tn Antigens.
417 *Biomolecules* **5**, 1783-1809 (2015).
418 29. E. Rodriguez *et al.*, Fasciola hepatica Immune Regulates CD11c+ Cells by Interacting with the
419 Macrophage Gal/GalNAc Lectin. *Front Immunol* **8**, 264 (2017).
420 30. S. K. Singh *et al.*, Characterization of murine MGL1 and MGL2 C-type lectins: distinct glycan
421 specificities and tumor binding properties. *Mol Immunol* **46**, 1240-1249 (2009).
422 31. Y. Kumamoto, T. Hirai, P. W. Wong, D. H. Kaplan, A. Iwasaki, CD301b+ dendritic cells suppress T
423 follicular helper cells and antibody responses to protein antigens. *Elife* **5**, (2016).
424 32. Y. Kumamoto *et al.*, CD301b(+) dermal dendritic cells drive T helper 2 cell-mediated immunity.
425 *Immunity* **39**, 733-743 (2013).
426 33. J. A. Kenkel *et al.*, An Immunosuppressive Dendritic Cell Subset Accumulates at Secondary Sites
427 and Promotes Metastasis in Pancreatic Cancer. *Cancer Res* **77**, 4158-4170 (2017).
428 34. V. da Costa *et al.*, The Tn antigen promotes lung tumor growth by fostering immunosuppression
429 and angiogenesis via interaction with Macrophage Galactose-type lectin 2 (MGL2). *Cancer Lett*
430 **518**, 72-81 (2021).
431 35. E. C. Rosser, C. Mauri, Regulatory B cells: origin, phenotype, and function. *Immunity* **42**, 607-612
432 (2015).
433 36. A. Mizoguchi, E. Mizoguchi, R. N. Smith, F. I. Preffer, A. K. Bhan, Suppressive role of B cells in
434 chronic colitis of T cell receptor alpha mutant mice. *J Exp Med* **186**, 1749-1756 (1997).
435 37. C. Mauri, D. Gray, N. Mushtaq, M. Londei, Prevention of arthritis by interleukin 10-producing B
436 cells. *J Exp Med* **197**, 489-501 (2003).
437 38. Y. Jiao *et al.*, Regulatory B cells correlate with HIV disease progression. *Microbiol Immunol* **58**,
438 449-455 (2014).
439 39. J. Liu *et al.*, IL-10-producing B cells are induced early in HIV-1 infection and suppress HIV-1-
440 specific T cell responses. *PLoS One* **9**, e89236 (2014).
441 40. Y. Zhang, R. Morgan, E. R. Podack, J. Rosenblatt, B cell regulation of anti-tumor immune
442 response. *Immunol Res* **57**, 115-124 (2013).
443 41. X. Zhou, Y. X. Su, X. M. Lao, Y. J. Liang, G. Q. Liao, CD19(+)IL-10(+) regulatory B cells affect survival
444 of tongue squamous cell carcinoma patients and induce resting CD4(+) T cells to CD4(+)Foxp3(+)
445 regulatory T cells. *Oral Oncol* **53**, 27-35 (2016).
446 42. M. Shen, J. Wang, X. Ren, New Insights into Tumor-Infiltrating B Lymphocytes in Breast Cancer:
447 Clinical Impacts and Regulatory Mechanisms. *Front Immunol* **9**, 470 (2018).
448 43. L. Ye *et al.*, Tumor-derived exosomal HMGB1 fosters hepatocellular carcinoma immune evasion
449 by promoting TIM-1(+) regulatory B cell expansion. *J Immunother Cancer* **6**, 145 (2018).
450 44. F. Burke, A. J. Stagg, P. A. Bedford, N. English, S. C. Knight, IL-10-producing B220+CD11c- APC in
451 mouse spleen. *J Immunol* **173**, 2362-2372 (2004).
452 45. S. Fillatreau, C. H. Sweenie, M. J. McGeachy, D. Gray, S. M. Anderton, B cells regulate
453 autoimmunity by provision of IL-10. *Nat Immunol* **3**, 944-950 (2002).
454 46. K. Yanaba *et al.*, A regulatory B cell subset with a unique CD1dhiCD5+ phenotype controls T cell-
455 dependent inflammatory responses. *Immunity* **28**, 639-650 (2008).

456 47. F. Flores-Borja *et al.*, CD19+CD24hiCD38hi B cells maintain regulatory T cells while limiting TH1
457 and TH17 differentiation. *Sci Transl Med* **5**, 173ra123 (2013).
458 48. X. Liu *et al.*, B cells expressing CD11b effectively inhibit CD4+ T-cell responses and ameliorate
459 experimental autoimmune hepatitis in mice. *Hepatology* **62**, 1563-1575 (2015).
460 49. S. A. Geherin *et al.*, IL-10+ Innate-like B Cells Are Part of the Skin Immune System and Require
461 alpha4beta1 Integrin To Migrate between the Peritoneum and Inflamed Skin. *J Immunol* **196**,
462 2514-2525 (2016).
463 50. E. E. Ghosn, Y. Yang, J. Tung, L. A. Herzenberg, L. A. Herzenberg, CD11b expression distinguishes
464 sequential stages of peritoneal B-1 development. *Proc Natl Acad Sci U S A* **105**, 5195-5200 (2008).
465 51. J. B. Wong *et al.*, B-1a cells acquire their unique characteristics by bypassing the pre-BCR
466 selection stage. *Nat Commun* **10**, 4768 (2019).
467 52. T. Kobayashi *et al.*, Regulatory B1a Cells Suppress Melanoma Tumor Immunity via IL-10
468 Production and Inhibiting T Helper Type 1 Cytokine Production in Tumor-Infiltrating CD8(+) T
469 Cells. *J Invest Dermatol* **139**, 1535-1544 e1531 (2019).
470 53. D. O. Griffin, T. L. Rothstein, Human "orchestrator" CD11b(+) B1 cells spontaneously secrete
471 interleukin-10 and regulate T-cell activity. *Mol Med* **18**, 1003-1008 (2012).
472 54. M. Kanayama *et al.*, Myeloid-like B cells boost emergency myelopoiesis through IL-10 production
473 during infection. *J Exp Med* **220**, (2023).
474 55. X. Zhang, Regulatory functions of innate-like B cells. *Cell Mol Immunol* **10**, 113-121 (2013).
475 56. T. Ju, R. D. Cummings, A unique molecular chaperone Cosmc required for activity of the
476 mammalian core 1 beta 3-galactosyltransferase. *Proc Natl Acad Sci U S A* **99**, 16613-16618 (2002).
477 57. Y. Matsumoto *et al.*, Identification of Tn antigen O-GalNAc-expressing glycoproteins in human
478 carcinomas using novel anti-Tn recombinant antibodies. *Glycobiology* **30**, 282-300 (2020).
479 58. G. J. Rowse, R. M. Tempero, M. L. VanLith, M. A. Hollingsworth, S. J. Gendler, Tolerance and
480 immunity to MUC1 in a human MUC1 transgenic murine model. *Cancer Res* **58**, 315-321 (1998).
481 59. S. Cascio, A. M. Farkas, R. P. Hughey, O. J. Finn, Altered glycosylation of MUC1 influences its
482 association with CIN85: the role of this novel complex in cancer cell invasion and migration.
483 *Oncotarget* **4**, 1686-1697 (2013).
484 60. O. J. Finn *et al.*, Importance of MUC1 and spontaneous mouse tumor models for understanding
485 the immunobiology of human adenocarcinomas. *Immunol Res* **50**, 261-268 (2011).
486 61. D. K. Kadayakkara *et al.*, Inflammation driven by overexpression of the hypoglycosylated
487 abnormal mucin 1 (MUC1) links inflammatory bowel disease and pancreatitis. *Pancreas* **39**, 510-
488 515 (2010).
489 62. S. O. Ryan, A. M. Vlad, K. Islam, J. Gariepy, O. J. Finn, Tumor-associated MUC1 glycopeptide
490 epitopes are not subject to self-tolerance and improve responses to MUC1 peptide epitopes in
491 MUC1 transgenic mice. *Biol Chem* **390**, 611-618 (2009).
492 63. M. D. Burdick, A. Harris, C. J. Reid, T. Iwamura, M. A. Hollingsworth, Oligosaccharides expressed
493 on MUC1 produced by pancreatic and colon tumor cell lines. *J Biol Chem* **272**, 24198-24202
494 (1997).
495 64. B. T. Hofmann *et al.*, COSMC knockdown mediated aberrant O-glycosylation promotes oncogenic
496 properties in pancreatic cancer. *Mol Cancer* **14**, 109 (2015).
497 65. C. B. Madsen *et al.*, Glycan elongation beyond the mucin associated Tn antigen protects tumor
498 cells from immune-mediated killing. *PLoS One* **8**, e72413 (2013).
499 66. N. Baumgarth, B-1 Cell Heterogeneity and the Regulation of Natural and Antigen-Induced IgM
500 Production. *Front Immunol* **7**, 324 (2016).
501 67. N. Rodriguez-Zhurbenko, T. D. Quach, T. L. Rothstein, A. M. Hernandez, Human B-1 cells are
502 important contributors to the naturally-occurring IgM pool against the tumor-associated
503 ganglioside Neu5GcGM3. *Front Immunol* **13**, 1061651 (2022).

504
505

506 **ACKNOWLEDGEMENTS**

507 We acknowledge the following individuals for contributing transgenic mice, cell lines, and
508 monoclonal antibodies: Dr. Akiko Iwasaki, Dr. Richard Cummings, Dr. Kebin Liu, Dr. Sarah
509 Gendler. National Institutes of Health grants R01AI123383, R01AI152766, and R41AI157287
510 supported this work.

511

512 **Figure legends:**

513 **Fig. 1. Tumor growth and CD301b expression in Tn^{lo} and Tn^{hi} breast cancer models.** AT3
514 (Tn^{lo}) and AT3 cosmc KO cells (Tn^{hi}) (2.5E5/mouse) were injected into the mammary pads of
515 C57BL/6 mice (n = 25). Tumor sizes were monitored. **A.** Tumor sizes were calculated based on
516 (length times $width^2$)/2 for volumes in mm^3. **B-C.** Tumor-free and tumor-bearing mice were
517 euthanized, and tissues were obtained from spleens, lymph nodes, bone marrow, and tumors. Flow
518 cytometry was performed to assess immune profiles. CD45+ cells were gated from total
519 mononuclear cells (FSC/SSC) and viable cells according to the gating strategy in Supplementary
520 Fig. 2. CD301b+ cells were then gated from CD45+ cells and assessed in tumor-free and tumor-
521 bearing tissues.

522

523 **Fig. 2. Characterization of CD45+CD301b+ immune cells.** Tn^{hi} AT3 tumor-bearing mice were
524 euthanized, and tumor tissues were harvested. Single-cell suspensions were stained for indicated
525 immune cell markers. CD45+CD301b+ immune cells were gated according to fluorescence minus
526 one (FMO) plus isotype staining controls (Supplementary Fig. 2) in: **A-C.** CD45+CD301b+ cells
527 were gated in Tn^{hi} tumor tissues, and immune cell populations (B220, CD19, CD11c, CD11b, CD3,
528 NK1.1) were assessed compared to indicated controls. **D.** Quantification of A-C**. E.** Gated
529 $CD45^+CD301b^+B220^+CD19^+$ cells were assessed for CD11c and CD11b. F. Comparison between
530 the total numbers of $CD45^+B220^+CD19^+$ cells, $CD45^+B220^+CD19^+CD301b^+$ cells, and all other
531 $CD45^+$ cells in Tn^{hi} and Tn^{lo} tumors per mg of tumor.

532

533 **Fig. 3. Phenotypes of Tn^{hi} tumor-infiltrating $CD45^+CD301b^+$ B cells.** Tn^{hi} AT3 tumor-bearing
534 mice were euthanized, and tumor tissues were harvested. Single-cell suspensions were stained for
535 indicated immune cell markers. **A-E.** $CD45^+CD301b^+$ B cells ($B220^+CD19^+$) were gated according
536 to FMO) plus isotype staining controls (Supplementary Fig. 2) and assessed for the presence of the
537 surface proteins associated with regulatory B cells **F.** Quantification of **A-E**. **G.** Mean fluorescent
538 intensity (MFI) of CD301b was assessed in gated $CD45^+B220^+CD19^+$ cells infiltrating Tn^{lo} and
539 Tn^{hi} tumors **H**. Splenocytes were obtained from tumor-free C57BL/6 mice. Cells were unselected,
540 positively selected for $CD19^+$ cells, or negatively isolated based on pan B cell markers (please see
541 Supplementary Fig. 3 for cell purity). Each splenocyte sample was co-cultured with or without Tn^{hi}
542 or Tn^{lo} AT3 tumor cells for three days. Flow cytometry was used to analyze $CD301b^+$ expression
543 in $CD45^+B220^+CD19^+$ cells. Indicated values represent the mean fluorescent intensity of $CD301b^+$.

544

545 **Fig. 4**. **Tumor growth is attenuated in a B cell-deficient mouse model.** Tn^{hi} tumors were injected
546 into the mammary pads of WT or RAG KO mice. Tumor growth was **A.** monitored. When tumor
547 sizes reached a maximum dimension of 1.2 cm, tumor tissues were collected, and **B-C** analyzed for
548 CD301b+ immune cell infiltration. **D.** Total numbers of CD45+B220+CD19+ cells in Tn^{hi} tumors
549 in WT C57BL/6 and RAG KO mice per mg of the tumor.

550

551 **Fig. 5. Tn-associated Regulation by $CD45^+CD301b^+$ tumor-infiltrating immune cells. A-B**
552 AT3 Tn^{hi} (cosmc KO) cells (2.5E5/mouse) were injected into the mammary pad in 4-6 mice per
553 group. Mice were euthanized, and tumors were processed for single-cell suspensions. Cells were
554 stained for extracellular markers, and intracellular staining was used to assess **A.** Mean Fluorescent
555 Intensity (MFI) and **B.** % positive of indicated parent populations of cytokines IL10, IL35 (EBI3

556 subunit), IL35 (p35 subunit), and TGFβ in gated cell populations (please see our gating strategy in
557 Supplementary Fig.4).
558
559 **Fig. 6. Tumor growth in CD301b-depleted and Tn^{hi} breast cancer models. A.** Tn^{lo} (AT3) and
560 Tn^{hi} (AT3 cosmc KO) tumor cells ($2.5x10^5$/mouse) were injected into heterozygous MGL2-DTR
561 mice with or without $CD301b^+$ cells depleted (n= 4 or 5) mice per group into the mammary pad.
562 Tumor sizes were monitored. **B.** Tn^{hi} tumor cells ($2.5x10^5$/mouse) were injected into the mammary
563 pads of homozygous MGL2-DTR mice (n=5). Tumor sizes were monitored. **C**. Methylcholanthrene
564 (MCA) was injected into the mammary pads of WT C57BL/6 and MUC1.Tg (Tn^{hi}) mice to generate
565 spontaneous breast tumors. Survival of mice (tumor dimensions > 1.2cm) were monitored. **D.**
566 MCA-induced tumor tissues were obtained from mice, and flow cytometry was used to assess
567 $CD301b^+$ expression on tumor-infiltrating B cells.

A

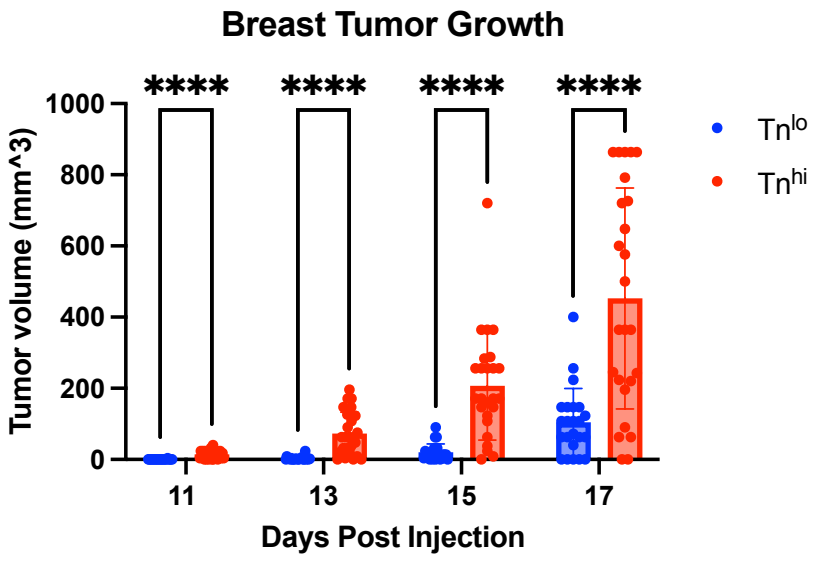
Breast Tumor Growth
****
****
****
****
Tumor volume (mm^3)
1000
800
600
400
200
0
11
13
15
17
Days Post Injection
Tn^lo
Tn^hi

B

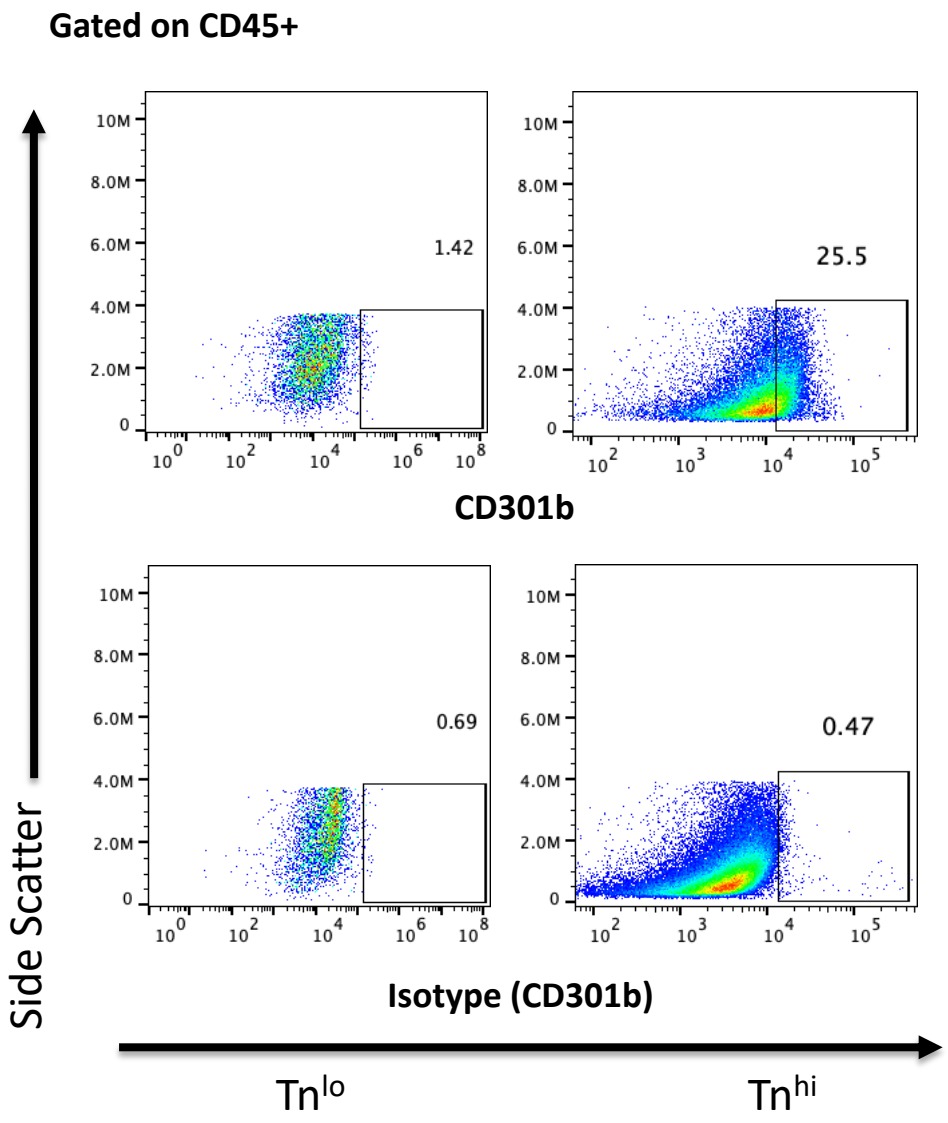
Gated on CD45+
1.42
25.5
CD301b
0.69
0.47
Isotype (CD301b)
Side Scatter
Tn^lo
Tn^hi

C

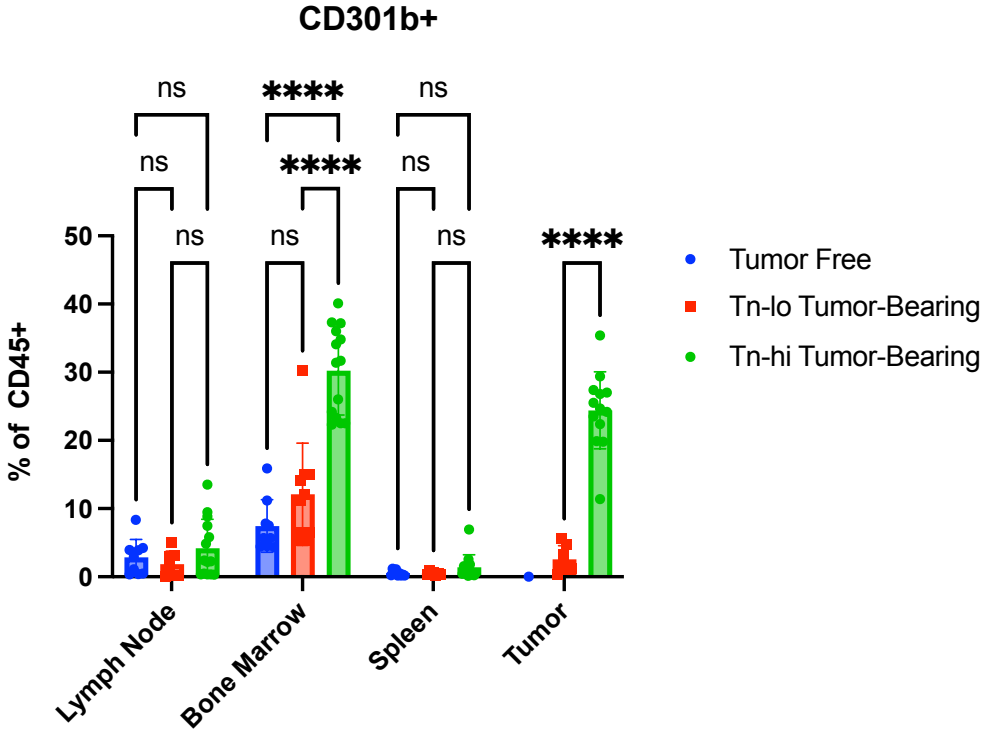
CD301b+
ns
****
ns
ns
****
ns
ns
ns
ns
****
% of CD45+
50
40
30
20
10
0
Lymph Node
Bone Marrow
Spleen
Tumor
Tumor Free
Tn-lo Tumor-Bearing
Tn-hi Tumor-Bearing

Tn^{hi} Tumor-infiltrating Gated on CD45+ CD301b+

A CD19+ B220+ B CD11c+ CD11b+ C CD3+ NK1.1+

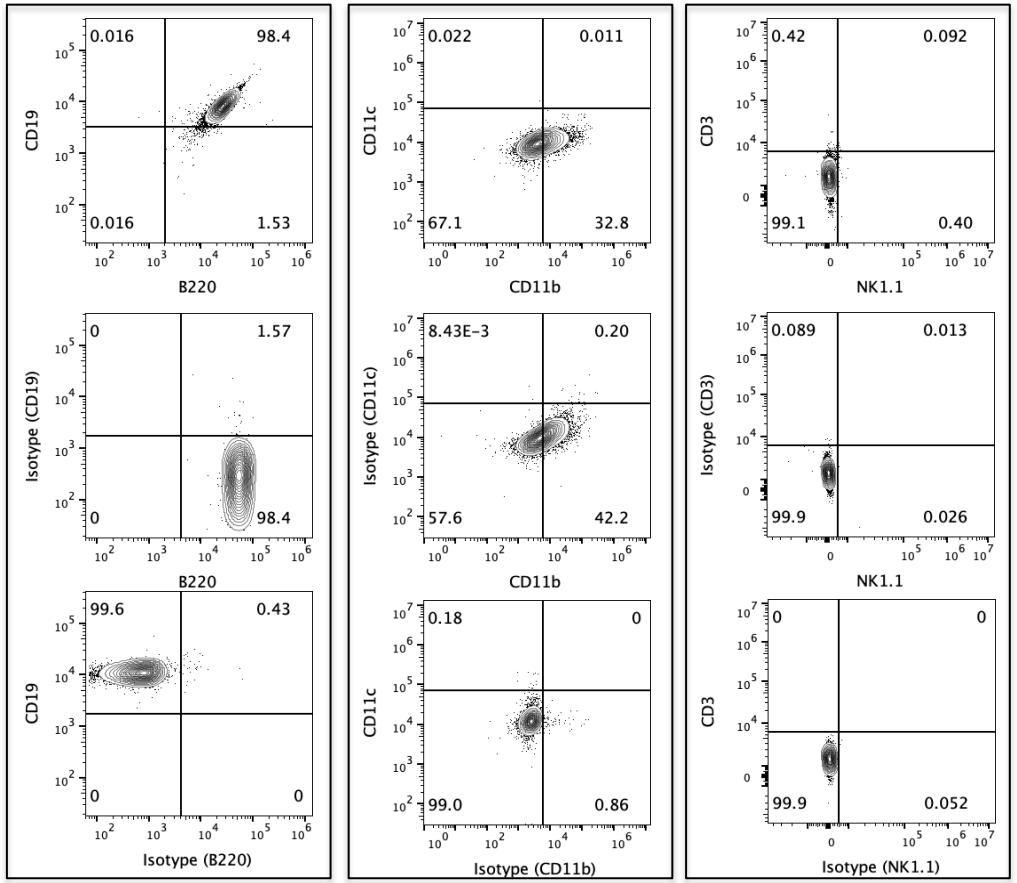

E Tn^{hi} Tumor-infiltrating Gated on CD45+ CD301b+ B220+ CD19+

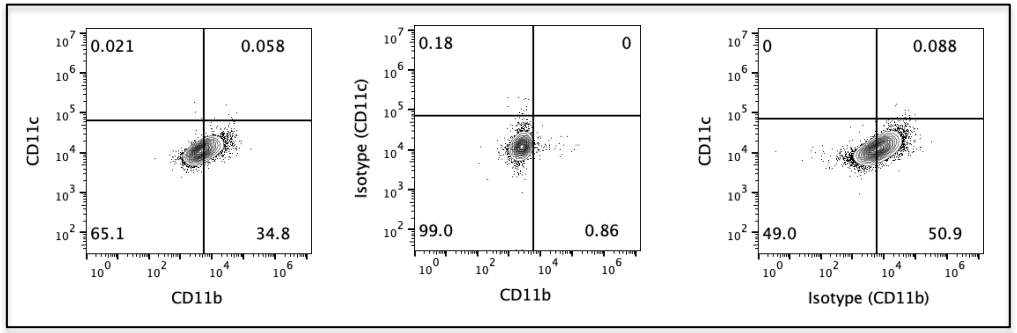

D

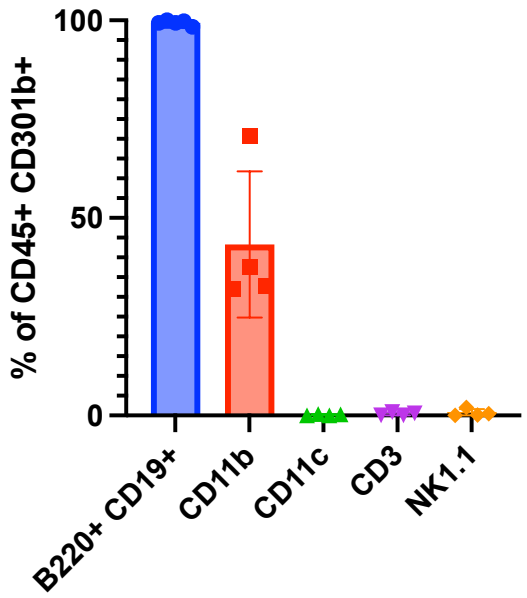

F

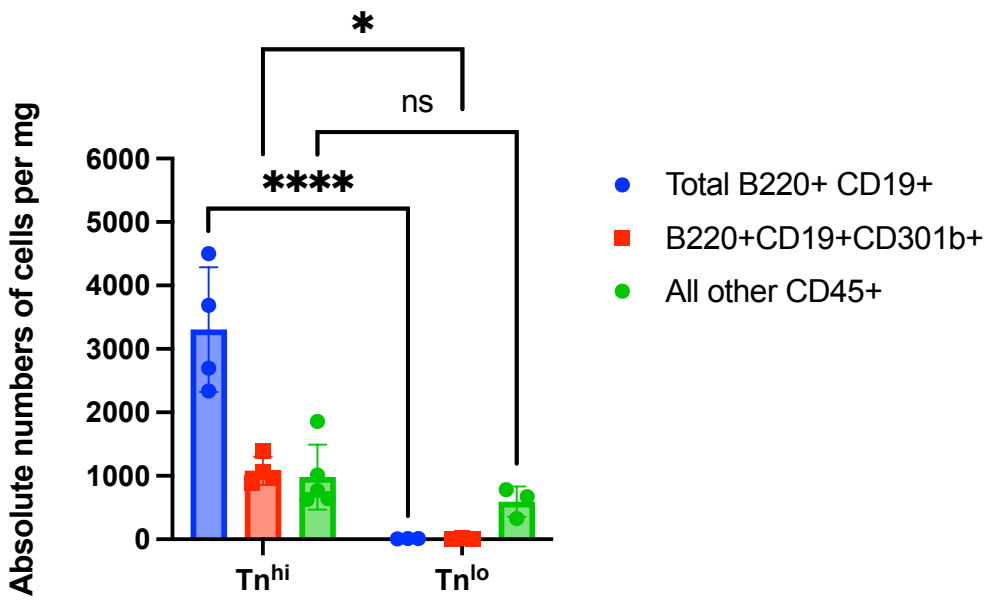

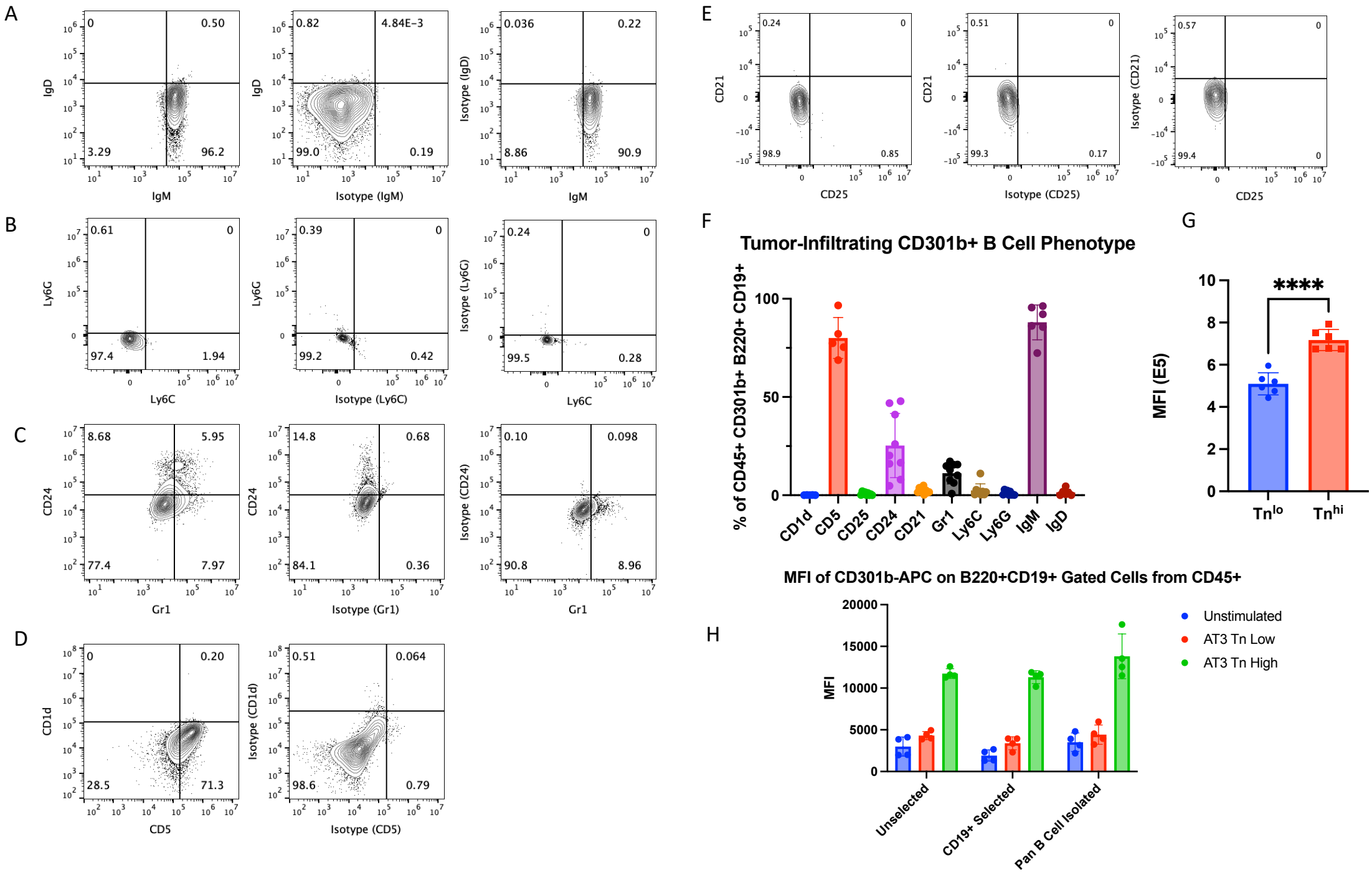
A
IgD
IgM
0
0.50
3.29
96.2
Isotype (IgM)
0.82
4.84E-3
99.0
0.19
Isotype (IgD)
0.036
0.22
8.86
90.9
B
Ly6G
Ly6C
0.61
0
97.4
1.94
Isotype (Ly6C)
0.39
0
99.2
0.42
Isotype (Ly6G)
0.24
0
99.5
0.28
C
CD24
Gr1
8.68
5.95
77.4
7.97
Isotype (Gr1)
14.8
0.68
84.1
0.36
Isotype (CD24)
0.10
0.098
90.8
8.96
D
CD1d
CD5
0
0.20
28.5
71.3
Isotype (CD5)
0.51
0.064
98.6
0.79
Isotype (CD1d)
E
CD21
CD25
0.24
0
98.9
0.85
Isotype (CD25)
0.51
0
99.3
0.17
Isotype (CD21)
0.57
0
99.4
0
F
Tumor-Infiltrating CD301b+ B Cell Phenotype
% of CD45+ CD301b+ B220+ CD19+
100
50
0
CD1d
CD5
CD25
CD24
CD21
Gr1
Ly6C
Ly6G
IgM
IgD
G
MFI (E5)
10
8
6
4
2
0
****
Tn^lo
Tn^hi
H
MFI of CD301b-APC on B220+CD19+ Gated Cells from CD45+
MFI
20000
15000
10000
5000
0
Unselected
CD19+ Selected
Pan B Cell Isolated
Unstimulated
AT3 Tn Low
AT3 Tn High

A

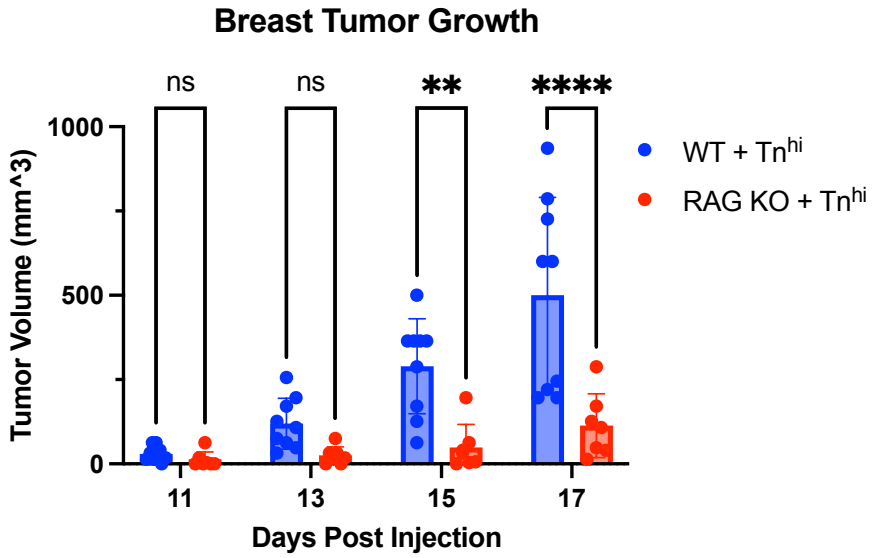
Breast Tumor Growth
ns
ns
**
****
1000
500
0
Tumor Volume (mm^3)
11
13
15
17
Days Post Injection
WT + Tn^hi
RAG KO + Tn^hi

C

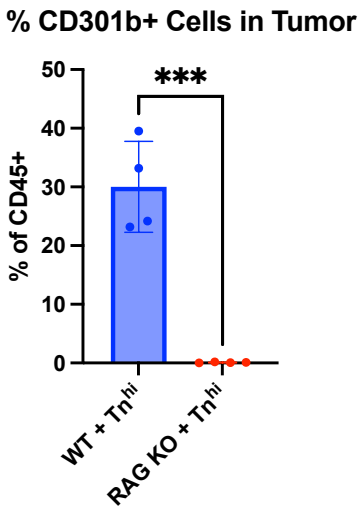
% CD301b+ Cells in Tumor
***
50
40
30
20
10
0
% of CD45+
WT + Tn^hi
RAG KO + Tn^hi

B

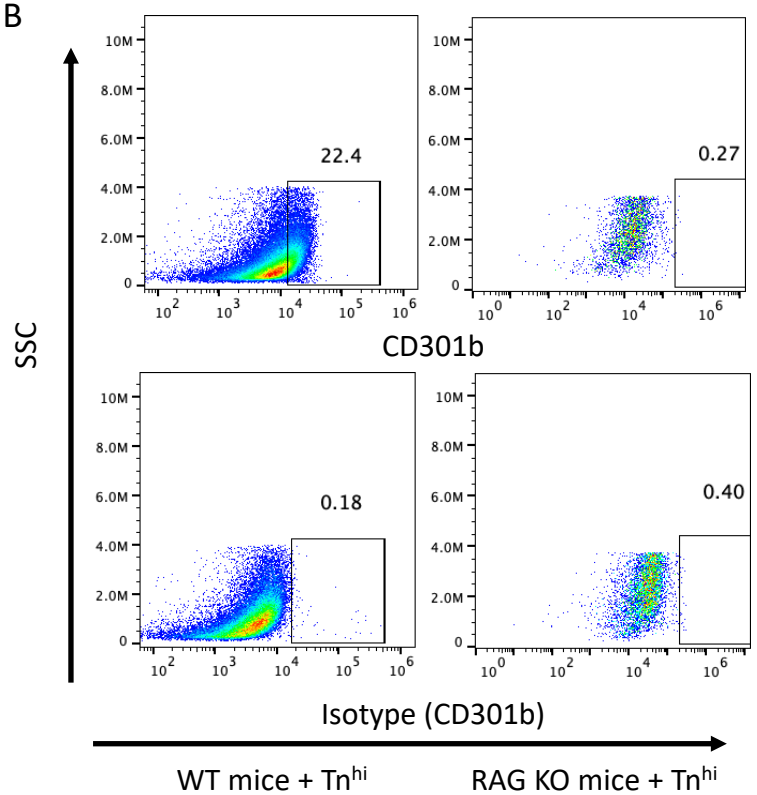
22.4
0.27
0.18
0.40
SSC
CD301b
Isotype (CD301b)
WT mice + Tn^hi
RAG KO mice + Tn^hi

D

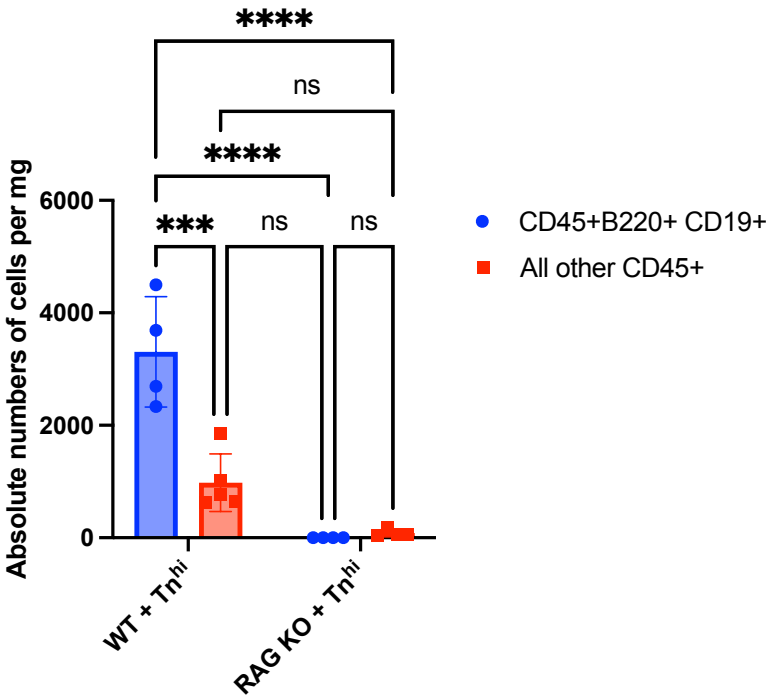
****
ns
****
***
ns
ns
6000
4000
2000
0
Absolute numbers of cells per mg
WT + Tn^hi
RAG KO + Tn^hi
CD45+B220+ CD19+
All other CD45+

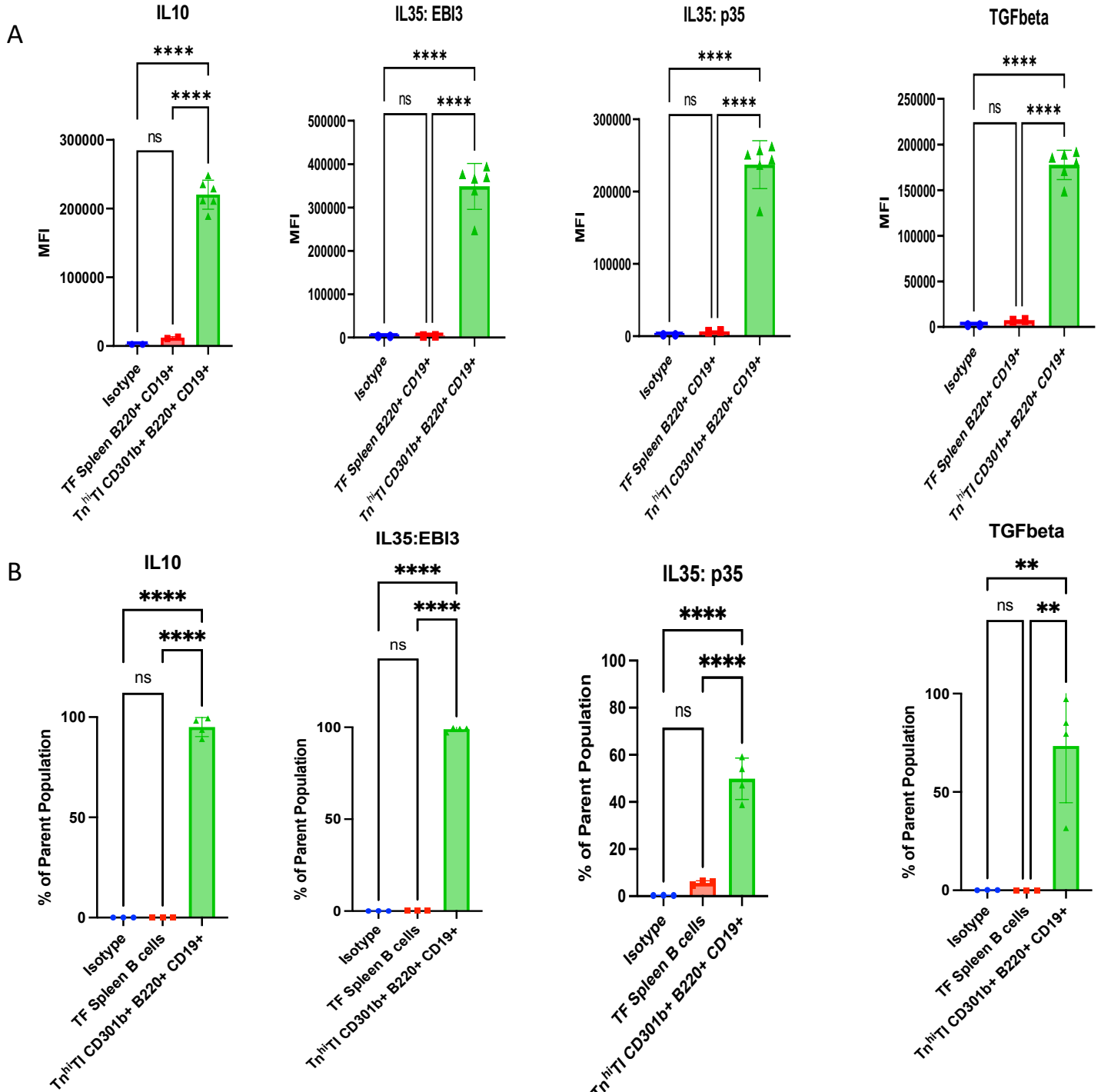
A
IL10
IL35: EBI3
IL35: p35
TGFbeta
MFI
****
ns
Isotype
TF Spleen B220+ CD19+
Tn hiTI CD301b+ B220+ CD19+
B
% of Parent Population
TF Spleen B cells
**

A

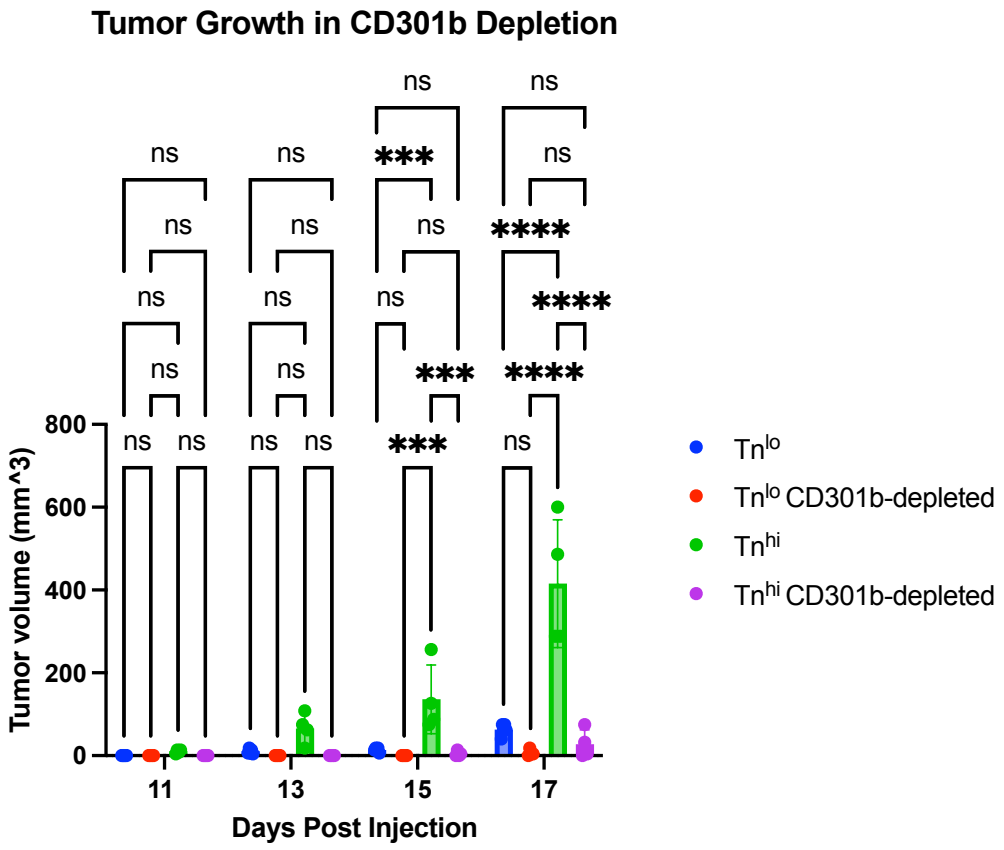
Tumor Growth in CD301b Depletion
Tumor volume (mm^3)
Days Post Injection
Tn^lo
Tn^lo CD301b-depleted
Tn^hi
Tn^hi CD301b-depleted

B

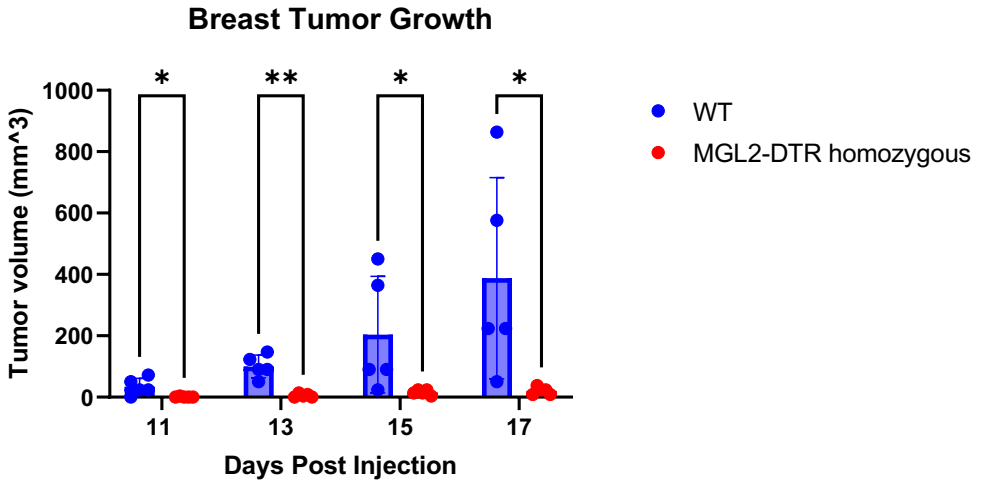
Breast Tumor Growth
Tumor volume (mm^3)
Days Post Injection
WT
MGL2-DTR homozygous

C

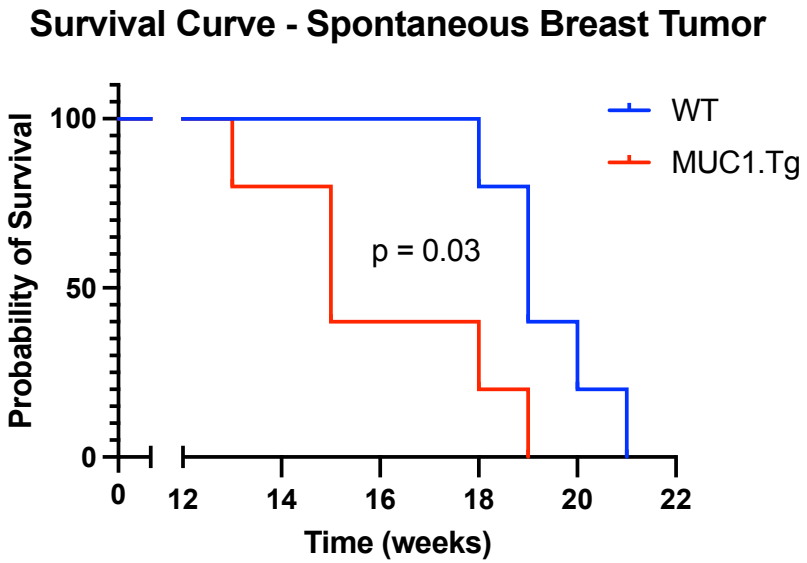
Survival Curve - Spontaneous Breast Tumor
Probability of Survival
Time (weeks)
p = 0.03
WT
MUC1.Tg

D

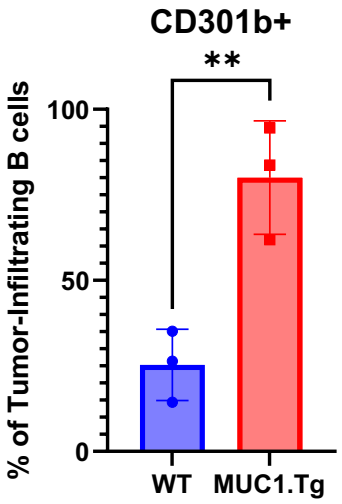
CD301b+
% of Tumor-Infiltrating B cells
WT
MUC1.Tg